

# On the Download Alleviation for the XV-15 Wing by Active Flow Control Using Large-Eddy Simulation

M. El-Alti<sup>1</sup>, P. Kjellgren, and L. Davidson

Division of Fluid Dynamics, Dept. of Applied Mechanics,  
Chalmers University of Technology, Gothenburg, Sweden  
`mohammad.el-alti@chalmers.se`

The flow around a XV-15 wing with and without active flow control (AFC) is investigated using large-eddy simulation (LES). Results show that a drag reduction of 34% is achieved with AFC.

## 1 Introduction

A part of the current flow control research at Chalmers University is directed towards vehicle aerodynamics optimization. The focus is on drag reduction using periodic excitation. As a first step in our research, we investigated the tilt-rotor XV-15 wing, which is a continuation of previous research [1, 2, 3]. The wing has a deflected flap at the trailing edge. The optimal angle is  $70^\circ$ , where the flow reattaches. If the deflection angle is increased, the flow separates and hence the download increases. With active flow control (AFC), the flow reattaches, the wake becomes narrower and the download is alleviated. In AFC the flow is controlled by supplying energy to the system. The energy input is provided in this study by an actuator that can blow in or suck out flow. The use of periodic excitation was shown to be more effective than steady blowing or suction [3]. Periodic excitation depends on many parameters that must be optimized. We have used the optimal values found in [1, 2] to analyze the download reduction process.

## 2 Numerical Method

The flow is computed by commercial finite-volume code, STAR-CD ver 4.02, with large-eddy simulation for solving the turbulent flow and the Smagorinsky SGS model. The Reynolds number is 130,000 based on the chord. The temporal discretization is a three-level, second-order scheme. Three different

schemes are investigated for the spatial discretization: a pure central difference scheme (CD), a blended central difference with upwind and finally a monotone advection and reconstruction scheme (MARS).

The configuration includes the wing with flap without rotors. At take-off, the wing is exposed by the flow from the rotors that yields the high download. The two-dimensional domain is span-wise extruded so that the span of the wing is 30% of its chord. The domain is shown in Figure 1.

The forcing is modeled as a transient velocity inlet, and the governing variables are the slot width, the velocity (both magnitude and direction) and the frequency. The RMS momentum from the slot is defined as

$$J_{rms} = \int \rho u_{rms}^2 dh = \rho u_{rms}^2 \Delta h \quad (1)$$

We have a constant spatial velocity profile at the slot.  $\Delta h$  is the effective slot width. Further, we define the momentum-coefficient as

$$C_\mu = \frac{J_{rms}}{c \frac{1}{2} \rho u_\infty^2} = \frac{u_{rms}^2 \Delta h}{c \frac{1}{2} u_\infty^2} \quad (2)$$

where  $c$  is the length of the chord. Thus the velocity out from the slot is given by

$$u_{rms} = \sqrt{\frac{C_\mu c u_\infty^2}{2 \Delta h}}, \quad u(t) = \sqrt{2} u_{rms} \sin(2\pi F t) \quad (3)$$

where  $F$  is the frequency. Finally, we define the non-dimensional forcing frequency as

$$F^+ = \frac{F \cdot X_{TE}}{U_\infty} \quad (4)$$

where  $X_{TE}$  is the distance from the slot to the trailing edge of the flap.

The mesh consists of around 700 000 unstructured quadrilateral cells in the  $xy$ -plane and structured hexahedral cells in the  $yz$ -plane. The mesh quality for the forced case at the flap is:  $n^+ = 0.8 - 11$ ,  $\Delta s^+ = 6 - 65$  and  $\Delta z^+ = 40 - 400$ . Where  $n^+$  and  $s^+$  denote normal and tangential due to the wall, respectively.

### 3 Results

Simulations were made with and without AFC. The following values of the different parameters were chosen. The free-stream velocity is  $U_\infty = 7 \text{ m/s}$ ,  $F^+ = 0.7$ , and the slot is located at 10% of the flap (see Figure 1),  $\alpha = 35^\circ$  denotes the forcing angle due to the flap surface,  $\Delta h = 2 \text{ mm}$  which gives  $C_\mu = 1.5\%$ .

The spatial scheme dependence was investigated. For the blended scheme, the blending factor chosen was 0.95, i.e. 95% CD and 5% UD.

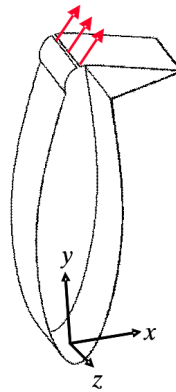


**Fig. 1.** The computational domain. Inlet at  $x = -6c$ ; outlet at  $x = 8c$ ; slip sidewalls at  $y = -6c$  and  $y = 7c$ .

### 3.1 Drag and lift

The predicted drag for the unforced case is in good agreement with experimental results and previous FEM computations [1, 2]. The normalized drag for the unforced case is 0.99. The experimental value is 1.03 [1]. This is the case for the pure CD scheme; however, this scheme showed wiggles in the region upstream of the wing. The MARS scheme over-predicted the drag to be 1.52, and the blended CD scheme also over-predicted to be 1.27. These two latter schemes however removed the wiggles. The predicted drag for the forced case is also in good agreement with the experimental results and previous FEM computations. The normalized drag is 0.76 for the pure CD scheme, compared with the experimental value of 0.73 [1]. We did not run the forced case with the MARS-scheme due to the high over-prediction. However, for the blended scheme, the normalized drag is 0.84.

The results below were all obtained with the blended scheme. In the drag and lift history plots in Figure 2, we can see that there are large fluctuations for the unforced case and that the peak to peak value is reduced with forcing. This is confirmed by calculating the RMS of the drag coefficient. The RMS of  $C_D$  is 0.29 and 0.14 for the unforced and forced case, respectively. We can also see that the drag history is modulated for the forced case. This is the actuation frequency, which is higher than the vortex shedding frequency. We can also see that the lift increases with forcing.

### 3.2 Pressure coefficient distribution and its RMS

Figure 3(a) plots the non dimensional pressure coefficient  $C_{p,x}$  obtained by using the projection of the pressure load in the  $x$ -direction for both the upper and lower wing surfaces.  $C_{p,x}$  is investigated because it is the quantity that

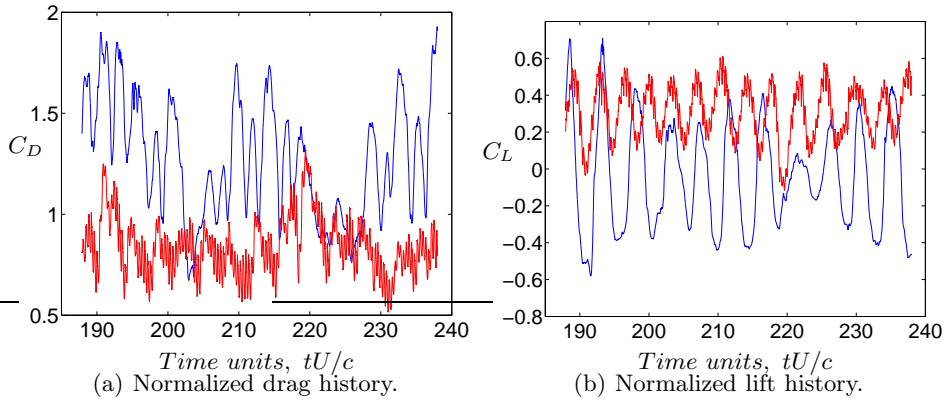


**Fig. 2.** Time histories of drag and lift, — : AFC OFF; — : AFC ON.

contributes to the drag,  $C_D$ . High values of  $C_{p,x}$  are found at the upper surface where the flow impinges on the wing.  $C_{p,x}$  however decreases a great deal at the curvature connecting the flap and becomes negative. The comparison of the pressure coefficient distribution with the unforced case shows that a strong reduction is obtained at the flap surface. The reduction of pressure is a result of the flow reattachment mechanism due to AFC. We also observe that the peak values are reduced in the RMS plot in Figure 3(b), which is the reduction of peak to peak value of drag history for the AFC case, see Figure 2(a).

At the lower surface, the pressure coefficient is higher with AFC than without. This confirms that, in the mean, the base pressure has increased with forcing. The high base pressure with AFC covers the entire lower surface, and is probably a side-effect of the reduction done on the flap surface. We observe from the RMS of  $C_{p,x}$  in figure 3(b) that the main reduction in peak to peak in  $C_D$  is caused by the lower surface.

### 3.3 Mean velocity, pressure and resolved kinetic energy

Figures 4(a) and 4(b) show contour plots of the time average of the  $x$ -component of velocity together with streamlines. For the unforced case, we observe a large separation region along the flap and a large wake region. We also observe that there is a large region with negative velocities (dark blue) behind the wing in the unforced case. With AFC, the large separation on the flap region is removed (i.e. the flow is reattached in the mean), the wake size narrows a great deal and the region with negative velocities behind the wing is smaller. The wake structures become smaller.

The resolved turbulent kinetic energy (KE) is shown in Figures 4(c) and 4(d) as contour plots. There are three main achievements with forcing in this state. We observe a high KE region on the flap, creating low pressure and thus sucking the flow onto the surface, hence reattaching the flow. We also observe

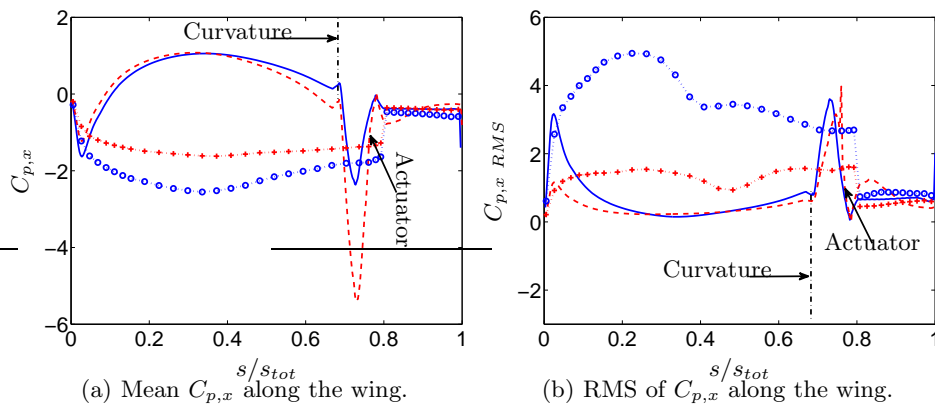


**Fig. 3.** Upper surface: — : AFC OFF; - - - : AFC ON, Lower surface: . . o . . : AFC OFF; . . + . . : AFC ON.

the huge decrease of KE in the wake due to forcing. The vortex shedding has been destroyed so that the wake is less intense. Further, the wake is narrower and smaller.

## 4 Conclusion

An XV-15 wing with a flap was investigated with and without AFC. Results show that a drag reduction by 34% is achieved with AFC. The reduction is due to flow reattachment on the flap surface, which gave rise to a less intensive wake with smaller wake structures and a narrower wake.

## 5 Acknowledgements

This work is supported by the **Swedish Agency of Innovation Systems (VINNOVA)**, **Volvo 3P**, **SKAB** and **CD-ADAPCO**. Financial support by SNIC (the Swedish National Infrastructure for Computing) for computer time at C3SE (Chalmers Centre for Computational Science and Engineering) is gratefully acknowledged.

## References

1. P. Kjellgren, A. Hassan, J. Sivasubramanian, L. Cullen, D. Cerchie, and I. Wygan-ski. Download alleviation for the xv-15: computations and experiments of flows around the wing. In *Biennial International Powered Lift Conference and Exhibit*, Williamsburg, Virginia, Nov 5-7 2002.

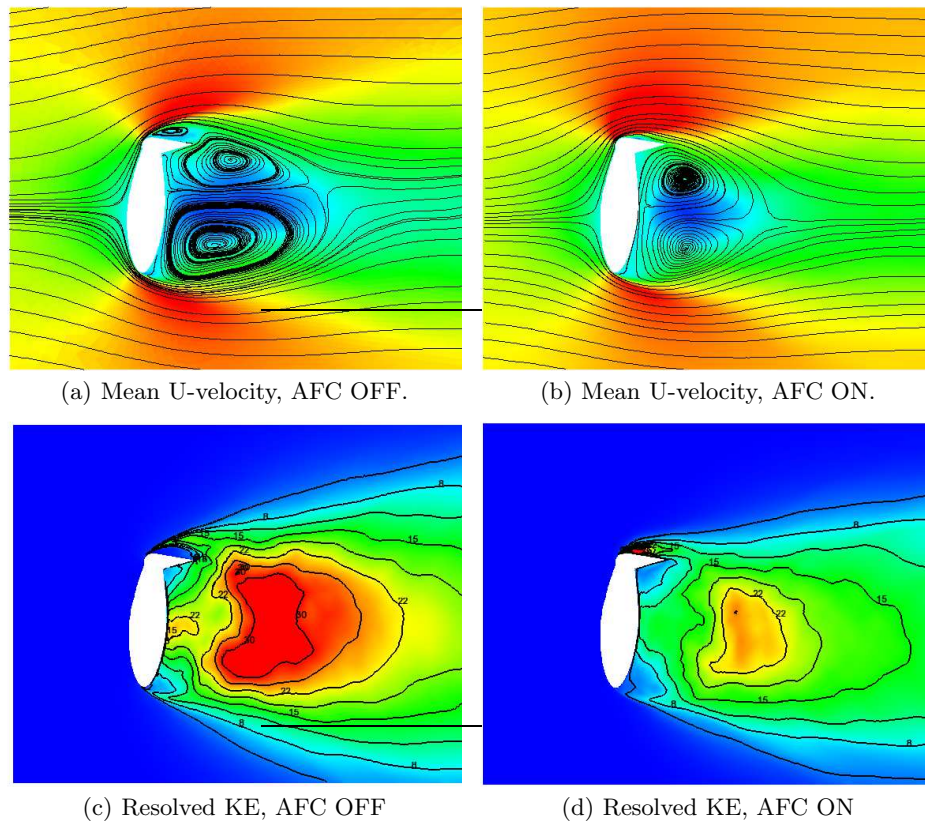


**Fig. 4.** Mean U-velocity with streamlines (top) and resolved turbulent kinetic energy (bottom).

2. P. Kjellgren, D. Cerchie, L. Cullen, and I. Wyganski. Active flow control on bluff bodies with distinct separation locations. In *1st Flow Control Conference*, St. Louis, Missouri, June 24-26 2002.
3. P. Kjellgren, N. Anderberg, and I. Wyganski. Download alleviation by periodic excitation on a typical tilt-rotor configuration - computation and experiment. In *Fluids 2000 Conference and Exhibit*, Denver, CO, June 19-22 2000.